Distribution Agreement

Signature:

Xinzhu Wang Date

Approval Sheet

Prediction of CBC Hemoglobin Levels for Preterm Infants: Evaluation of Anatomic Regions for Smartphone Photos

By

Xinzhu Wang

Master of Science in Public Health

Department of Biostatistics and Bioinformatics

Amita Manatunga, Ph.D.
Committee Chair

Jeong Hoon Jang, Ph.D.
Committee Member

Date

Abstract Cover Page

Prediction of CBC Hemoglobin Levels for Preterm Infants: Evaluation of Anatomic Regions for Smartphone Photos

By

Xinzhu Wang

B.S., University of Wisconsin - Madison, 2020

Thesis Committee Chair: Amita Manatunga, Ph.D.

An abstract of

A thesis submitted to the Faculty of the

Rollins School of Public Health of Emory University

in partial fulfillment of the requirements for the degree of

Master of Science in Public Health

in Department of Biostatistics and Bioinformatics

2022

Abstract

Prediction of CBC Hemoglobin Levels for Preterm Infants: Evaluation of Anatomic Regions for Smartphone Photos

By Xinzhu Wang

Anemia is a condition in which the body's red blood cell count is lower than normal and become unable to provide enough oxygen to the tissues. If untreated, it leads to a delay in brain maturation, tissue hypoxia, and growth impairment. The routine techniques to detect anemia are blood laboratory tests such as complete blood count (CBC). These tests require frequent blood draws, which may cause phlebotomy-induced complications or exacerbate the existing anemia.

Non-invasive technologies are needed for preterm infants to quantitatively estimate their hemoglobin levels and thereby monitoring the anemia status. Inspired by a recent study using smartphone photos of adults' fingernail beds for non-invasive detection of anemia, we aim to explore whether a non-invasive method that is similar to this smartphone image analysis algorithm can be developed for the preterm infants. The goal of this study is to investigate several anatomic regions and to determine smartphone photos of which anatomic region (fingernail, palm or toenail) can most accurately reflect the preterm infants' CBC Hgb levels. Linear regression models are fitted to predict the hemoglobin outcomes for all anatomic regions as well as individually for each anatomic region. Mean squared errors and mean absolute errors for all models across all testing data are calculated to compare the prediction performance.

The anatomic region is significantly associated with the CBC Hgb levels, indicating that different anatomic regions have different intercepts for the regression equation. The mean predicted Hgb levels at palm region is significantly different from the mean predicted Hgb levels at fingernail region (p-value = 0.028). The regression model for all anatomic regions has a mean absolute error of 1.26 and mean squared error of 2.53 based on the testing data that includes all anatomic regions. The higher MSE and absolute errors are found with palm and fingernail testing data while the error is slightly smaller for the toenail testing data.

Depending on the anatomic regions, the predictive equations can be different. The regression equation that includes all anatomic regions appear to have similar prediction errors across all anatomic regions, but the toenail testing data may provide slightly smaller prediction errors compared with the fingernail testing data and palm testing data.

Keywords – non-invasive anemia detection, smartphone photo, anatomic region, prediction accuracy

Cover Page

Prediction of CBC Hemoglobin Levels for Preterm Infants: Evaluation of Anatomic Regions for Smartphone Photos

By

Xinzhu Wang

B.S., University of Wisconsin - Madison, 2020

Thesis Advisor: Amita Manatunga, Ph.D.

A thesis submitted to the Faculty of the
Rollins School of Public Health of Emory University
in partial fulfillment of the requirements for the degree of
Master of Science in Public Health
in Department of Biostatistics and Bioinformatics
2022

Acknowledgments

First and foremost, I would like to express my deep and sincere appreciation to my research supervisor, Dr. Amita Manatunga, Professor from Emory University Department of Biostatistics and Bioinformatics for giving me the opportunity to do research, providing invaluable guidance throughout my thesis work, and helping me on my PhD application.

I would like to thank Dr. Jeong Hoon Jang for being my reader and providing me with insightful comments.

I would like to thank Ms. Neeta Shenvi for her help with data management and coding. When I had any question, she always explained patiently. She also gave me a lot of useful comments on my thesis.

Also I express my thanks to Rachel Parker, PhD student worked with me in this project. She offered me many helps and gave me a lot of encouragements.

I am extremely grateful to my parents for their love, caring and support for educating and preparing me for the future. Special thanks to my boyfriend and all my friends for their love, understanding and accompany during the hard time because of the pandemic.

Last but not least, I would like to thank all the faculty members and staffs I met at Rollins. Thank you so much for your kind supports.

Contents

1 Introduction

Anemia has been recognized as a significant worldwide public health problem in infants because of its wide range of effect on neonatal health, including physical symptoms such as immune deficiency, growth impairment and behavioral and physical deficits [1]. It is a condition in which the infant's reticulocyte and nucleated red blood cell (RBC) counts diminish and become unable to provide enough oxygen to the tissues [2]. If not treated, severe anemia may impair organ function due to a lack of oxygen, causing hypoxic tissue injury [3]. Anemia can be diagnosed by various blood laboratory tests or imaging techniques such as complete blood count (CBC), reticulocyte count, iron profile, and peripheral blood smear [4]. While blood-based laboratory tests are important components for detecting anemia, excessive blood draws can cause consequences such as worsening of the existing anemia, phlebotomy-induced complications, and an increased number of packed red blood cell (pRBC) transfusions [5]. Thus, there is a need for non-invasive technologies to more quantitatively and officially diagnose and monitor anemia with greater accuracy Hgb values [6].

Mannino et al (2018) have developed a smartphone app to serve as a non-invasive anemia screening tool for adults that may replace the blood-based testing by estimating the blood hemoglobin concentration through analyzing the color and metadata of fingernail bed smartphone photos [6]. It is inspired by the fact that anemia may qualitatively correlate with subjective assessments of pallor in various anatomic regions of the patient's body, namely the fingernail beds and palmar creases [7]. The study is primarily restricted to adult patients with anemia of different etiologies as well as healthy subjects. Mannino et al developed an algorithm utilizing robust multi-linear regression based on a bisquare weighting algorithm to relate the image parameter data to CBC Hgb levels for each patient. Compared with the gold standard Hgb level test obtained via CBC, the algorithm achieved a strong predicting performance with a mean absolute error of 0.82, which presents a promising opportunity to monitor the patients' hemoglobin levels non-invasively and immediately [6].

However, it is unknown that whether the Hgb levels measured by the smartphone app in Mannino's study can represent the CBC Hgb level of other populations such as infants. Preterm infants are especially susceptible to the development of anemia due to the low storage iron concentration, short red blood cell half-life and rapid catch-up growth [1]. Research has also indicated that in preterm infants, phlebotomy ”overdraw” in excess of that requested by the hospital is one of the main causes for the anemia [10]. As a result, preterm infants will necessarily need a non-invasive method to remotely diagnose and monitor their anemia status with higher precision Hgb levels. Besides, infants' nails have many characteristics that are different from adults' nails. First, infants have a disorderly capillary network at birth, and the capillary loops will not be evident in all anatomical sites until 14-17 weeks of age [8]. Second, another study shows that due to intrauterine distress or physiological alterations during birth, 92% infants have Beau's lines appeared on their fingernails and disappear with growth before 14 weeks [9]. Third, infants' fingernail sizes are much smaller compared with adults' fingernails. Hence, such different characteristics of infants' fingernails compared to those of adults make it more difficult to use Mannino's smartphone image analysis algorithm to estimate the Hgb levels of infants.

Given the facts mentioned above, it would be meaningful to explore whether a non-invasive method that is similar to Mannino's smartphone image analysis algorithm can be developed for preterm infants to monitor their hemoglobin levels to prevent unnecessary blood loss that can lead to anemia. In the long term, our work will promote a successful development and implementation of a non-invasive smartphone imaging-based diagnostic tool that can replace the invasive phlebotomy procedures, ultimately enhancing the well-being of infants who require regular monitoring of hemoglobin level.

A prospective study was conducted among preterm infants to determine whether it is feasible to develop a non-invasive method that predicts the CBC Hgb levels based on the color and metadata extracted from smartphone images of various anatomic regions. But it remains unclear which anatomic region of the body (e.g., fingernail, toenail or palm) should be chosen to yield more reliable predictions of CBC Hgb levels. In this thesis, we aim to investigate several anatomic regions and to determine smartphone photos of which anatomic region (fingernail, palm or toenail) that can most accurately reflect the preterm infants' CBC Hgb levels.

2 Methods

2.1 Data Collection

Demographic Data Collection

A prospective, multi-center, observational birth-cohort study of red blood cell transfusion and digestive tract oxygenation in preterm infants was conducted by Dr. Cassandra Josephson from Emory University in Atlanta, Georgia. As a part of this study, 61 preterm infants were recruited from January 2017 to present. Parents or guardians provided written informed consent before enrollment of their infants into this study. All enrolled infants received follow-up from birth to 90 days, hospital discharge, transfer to a non-study affiliated hospital, or death. All preterm infants born at 3 level III neonatal intensive care units (NICUs) in Atlanta, Georgia, were assessed for eligibility. Two NICUs were academically affiliated (Grady Memorial Hospital and Emory University Hospital Midtown) and part of a single regional perinatal center. The other NICU was private and not academically affiliated (Northside Hospital). Inclusion criteria was birthweight less or equal to 1250 g and postnatal age of 7 days or less. Exclusion criteria were (1) infant unlikely to survive beyond 7 days of life based on the assessment by the treating neonatologist; (2) severe congenital abnormality; (3) receipt of transfusion before enrollment; or (4) maternal decision not to participate. Hemoglobin values, including the date of testing, were measured using blood samples collected via venous blood draw and recorded every week up to 13 weeks in the hospital.

Image Data Collection

To collect image data, a Samsung S21 with default settings was used to take photos for infants' different anatomic regions (e.g., left and right fingernails, palm and toenails) on the date within 24 hours of the hemoglobin testing date. Each infant image was paired with its corresponding laboratory assessed CBC Hgb measurement (gold standard). Photos of limited regions were taken since nurses took pictures with minimal disturbances. The photos were obtained with camera flash both on and off. Prior to imaging, the smartphone's camera's auto-focus and brightness adjustment were activated by tapping the screen. Each image was taken with the smartphone at a distance of 0.5 m from the subjects' anatomic regions to ensure consistency. Images were taken under constant lighting conditions and room illuminations.

Each infant photo was then processed by AnemoCheck Mobile developed by Dr. Robert Mannio [6] to extract 51x51 pixel matrices of red, green and blud (RGB) color intensity values, as well as image metadata including photo brightness and exposure time. Furthermore, each 51x51 pixel matrix of color intensity values was then converted to a single number by calculating its average of all 2601 pixel-specific numbers in that matrix. That is, each image has three corresponding numbers that describes its red, blue and green color intensities. Given that each individual takes multiple smartphone photos on different anatomic regions at each time point, we simplify the data by selecting one photo with best view at each time point for each anatomic region. Left and right directions are ignored (e.g., left and right fingernail are both regarded as fingernail).

2.2 Statistical Methods

Linear Regression Models

The covariates we consider for the regression model for predicting CBC Hgb levels include: mean intensity values of RGB colors (averaged over the corresponding 51x51 pixel matrix), image metadata (brightness value and exposure time) and demographic variables (anatomic region, mother's gestational weeks and infant's age in weeks). Here, anatomic regions (e.g., fingernail, palm, toenail) are coded as dummy variables. Exposure time variable is standardized to ensure it has similar scale with other variables. The standardized exposure time variable is used in all regression models. Two-way interactions between anatomic regions and each image data variable representing color and metadata are also tested.

Demographic variables (gender, race, mother's gestational weeks, and infants' birthweights) are described using descriptive statistics including proportions for categorical variables and mean, median, minimum, maximum and standard deviations for continuous variables. The longitudinal CBC Hgb levels are summarized using means and standard deviations and the number of pictures taken per anatomic region and across all anatomic regions are calculated for all infants. All longitudinal statistics are reported according to infants' ages since birth.

It is worth noticing that there is no predictive equation for predicting CBC Hgb levels based on the RGB color data and image metadata (brightness value, exposure time, etc.) for infant population. In order to evaluate which anatomic region represents CBC Hgb levels with highest accuracy, we develop regression equations for each anatomic region (fingernail data only, palm data only, toenail data only) and the whole data including all anatomic regions. Doing separate regression analysis for each anatomic region allows the error variance to differ across different anatomic regions.

Each data set for each anatomic region and the whole data set are divided by the ratio of approximately 70% to 30% for training and testing. Three linear regression models are fitted separately for each of the anatomic regions using their corresponding training data to predict the CBC Hgb outcomes based on mean intensity values of RGB colors, image metadata (brightness value and exposure time), and demographic variables (mother's gestational weeks and infant's age in weeks). The three models are referred to as ModelFingernail, ModelPalm and ModelToenail. Hereafter, for the model built based on the training data selected from the whole data, we include indicators representing the anatomic regions, as well as mean of RGB matrices, image meta data brightness values and exposure time, infant's age in days and mother's gestational weeks. This model is referred to as overall model. The prediction errors of the four models are reported across all four testing datasets (testing dataset from the whole data, and those for each of the three anatomic regions).

Summary Statistics for Evaluation of Prediction Errors

In these linear regression analyses, we compute prediction errors to evaluate the prediction accuracy. Each model's regression coefficients estimated from the training dataset are applied to all four testing data to obtain the predicted Hgb values. We quantify the prediction error using three statistics: mean squared errors (MSE), mean absolute errors (MAE), and the first quantile (Q1), median (Q2), and the third quantile (Q3) of absolute errors. For y_i, i = 1, ... n of sample size of each testing data, the mean squared error can be summarized as the mean of the squared differences between the Hgb value each model predicts and the measured CBC Hgb level on all instances of the testing dataset, that is

$$MSE = \sum_{i=1}^{n} (\hat{y}_i - y_i)^2$$

where $\hat{y}_i$ is the predicted Hgb levels and y_i is the observed CBC Hgb levels. The mean absolute error can be summarized as the mean of the absolute values of the difference between the Hgb value the model predicts and the measured CBC Hgb level on all instances of the testing dataset, that is

$$MAE = \sum_{i=1}^{n} |\hat{y}_i - y_i|$$

The first, second and third quantiles of absolute error (Q1, Q2, Q3) are the values under which 25th, 50th and 75th percentile of absolute errors in the testing data are found.

An important challenge in this study is the longitudinal nature of the data, where photos and other variables from the same subject are collected on multiple anatomic regions at multiple time points. Straightforward application of regression to this data set is not appropriate since the measurements of the same subject may be correlated, violating the error independence assumption in regression. More specifically, the standard errors for regression coefficients and their corresponding p-values are invalid. To overcome this situation, we consider a bootstrap approach. The bootstrapping method is repeated 1000 times to estimate the proper standard errors and p-values for all linear regression models.

3 Results

3.1 Descriptive Statistics

As of March 7, 2022, the study has enrolled a total of 61 infants. Given that the image data for three infants are missing, only 58 infants' data is kept. Demographic summary statistics are presented in Table 3.1. 62% of the infants are male and 43% are white. Mothers' gestational weeks varies from 22 weeks and 2 days to 31 weeks and 5 days with a mean gestational week of 27 weeks and 7 days and a standard deviation of 2 weeks and 1 day. Infants' birthweight ranges from 406 g to 1240 g, with a mean of 909 g and standard deviation of 215 g.

Each infant enrolled has their CBC Hgb levels measured upon enrolling and is recorded by their infant age in days and weeks. Longitudinal measurements of CBC Hgb levels are plotted for each subject according to their age in weeks (Figure 3.1). On average, as an infant's age increases the mean hemoglobin value decreases. Infants with blood hemoglobin measured at week 0 have an average of 14.3 g/dL, where those measured at week 1 have an average of 12.2 g/dL and 10.1 g/dL (the lowest value) at week 7. Table 3.3 summarizes the Hgb measurements, and the number of pictures taken per anatomic region in a longitudinal perspective by infant age in weeks. In general, infants have the most pictures taken at the age of week 1 and gradually have less pictures taken as they grow up across all anatomic regions.

For each infant, photos are collected across several anatomical regions including fingernail, toenail and palm. There are a total of 1,002 photos across all infants with an average of 17 photos per infant. After selecting only one best picture among all anatomical regions for each infant at each time point, the final dataset used for analysis included 208 photos from 58 infants. The distribution of photos varies by infant. The fingernail is the most photographed region, with 85 (41%) of infants having photos in this region across enrollment followed by 77 (38%) palm and 46 (22%) toenail photos. Table 3.2 provides the descriptive statistics of RGB color intensity variables and image metadata variables brightness value and exposure time across all anatomic regions and in the whole data set. Among all the pictures selected, red color intensity value has a mean of 170 (standard deviation is 25.3) followed by for green 114 (standard deviation is 30.9) and for blue at 104 (standard deviation is 32.1). The mean brightness value is 7.48 with a standard deviation of 1.04 and the mean exposure time is 0.0018 with a standard deviation of 0.000996. Among all anatomic regions, all red, green and blue color intensity variables have minimum standard deviations in the palm region, and brightness value and exposure time have the largest standard deviations in the fingernail region.

3.2 Prediction Results

The sample size of the whole data is 208, with a training size of 145 and testing size of 63. After splitting, the sample size of the data for fingernail region is 85, with a training size of 60 and testing size of 25. The sample size of the data for palm region is 77, with a training size of 54 and testing size of 23. The sample size of the data for toenail region is only 46, with a training size of 33 and testing size of 13. We first fit the regression model including all variables for the whole training data ($n = 145$). The regression coefficients as well as the bootstrapped standard errors and p-values for the overall model that includes all anatomic regions are displayed in Table 3.4. None of the two-way interactions between anatomic regions and image data variables is significant (all p-values > 0.05) (see Table A0.1 to A0.5). Anatomic region is significantly related to the CBC Hgb levels since the predicted mean Hgb levels for palm region is significantly different from the predicted mean Hgb levels for fingernail region (p-value = 0.028). Red and green colors as well as infant age in days and mother's gestational weeks are significantly associated with Hgb outcomes. Figure 3.2 shows the residual error versus the predicted Hgb levels for this model. The residual error is calculated by using predicted Hgb levels minus the measured CBC Hgb levels. Finger 3.2 indicates that fingernail region has more variability in terms of prediction.

The regression coefficients, the bootstrapped standard errors and p-values for the three region-specific models are shown in appendix table A0.6, A0.7 and A0.8. RGB and infant age in days are significant predictors of Hgb outcomes in the fingernail region. No variable is significant in predicting Hgb outcomes in palm and toenail regions. Table 3.5 summarizes the regression equation for all four models (ModelFingernail, ModelPalm, ModelToenail and overall model). We note that the training sample sizes are different across different anatomic regions.

Table 3.6 shows the prediction errors of ModelFingernail, ModelPalm, ModelToenail and overall model across all testing data. The ranges of MAE for ModelFingernail, ModelPalm and ModelToenail are 1.45-1.66, 1.28-1.46, and 1.50-2.18, respectively. The MAE of the Overall model is the smallest, ranging from 1.24 to 1.42. Similarly, the ranges of MSE for ModelFingernail, ModelPalm and ModelToenail are 3.35-4.89, 2.77-3.48, 3.89-6.78, respectively. The MSE of the overall model is the smallest, ranging from 2.53 to 2.65. The absolute errors are also visualized as boxplots and displayed in quantiles in Figure 3.3. The overall model performs reasonably well across all testing data, producing similar mean squared errors and absolute errors across all testing data. However, with toenail testing data, the prediction error appears to be slightly smaller compared to the other regions (see Figure 3.3).

4 Discussion

In this longitudinal, observational study, the hemoglobin outcomes are predicted using linear regression equations. Firstly, we performed a linear regression analysis with data from all three anatomic regions combined, with covariates including indicator of indicator of anatomic regions (fingernail, palm and toenail), average color intensity values, and other image metadata and demographic variables. The significance of all possible two-way interactions between anatomic regions and image data variables (color intensity values and image metadata) are tested. Secondly, separate regression analyses were conducted for each individual anatomic region, which allows for different error distributions for each region. MAEs, AEs, and MSEs of all models across all testing data were then calculated and compared to evaluate the prediction performance. It turned out that the model including all anatomic regions always had lower prediction error and better performance than the three individual region models. Anatomic region was significantly related to the CBC Hgb levels. Even the prediction errors across all anatomic regions were very close, the overall model has relatively smaller prediction errors for the toenail region.

There are also some limitations of this study. Linear regression methods are used to make predictions. But given the longitudinal feature of the data, linear regression models don't allow each individual infant to have his or her own mean response curve to explain how responses changes over time. In this case, mixed-effect models may be used in the future to provide greater flexibility analysis in correlated longitudinal data and model the covariance structures with random effects. Besides, our data has a relatively small sample size, and the sample size for each anatomic region is also unbalanced. Increasing the cohort size and maintaining balanced sample size for different anatomic regions can improve the accuracy of Hgb level estimation. Besides, we summarized the color data from a 51x51 matrix for each subject to a single mean value, which may lead to loss of structural information of the photos. Prediction methods that can keep the full color data may improve the prediction performance.

Tables

	Total Number of Infants (N = 58)
Gender	
Female	22 (37.9%)
Male	36 (62.1%)
Race	
Black	20 (34.5%)
White	25 (43.1%)
Asian	3 (5.2%)
Multiple Races	3 (5.2%)
Missing	7 (12.1%)
Mother's Gestational Weeks	
Mean (SD)	27.7 (2.1)
Median (Min, Max)	27.8 (22.2, 31.5)
Birthweight (g)	
Mean (SD)	909 (215)
Median (Min, Max)	911 (406, 1240)

SD: standard deviation

Table 3.1: Descriptive statistics of demographic information. The data consists of 58 unique infant individuals as of March 7th, 2022. Categorical variable is summarized by count (percentage) and continuous variables are summarized by mean (standard deviation) and median (minimum, maximum).

	Fingernail (N = 85)	**Palm (N = 77)**	**Toenail (N = 46)**	**Overall (N = 208)**
R				
Mean (SD)	172 (26.4)	168 (24.3)	170 (25.1)	170 (25.3)
Median	170	166	167	169
(Min, Max)	(100, 231)	(114, 224)	(112, 226)	(100, 231)
G				
Mean (SD)	123 (29.8)	103 (27.2)	117 (33.6)	114 (30.9)
Median	122	102	118	113
(Min, Max)	(60.8, 211)	(44.6, 185)	(59.1, 211)	(44.6, 211)
B				
Mean (SD)	112 (30.1)	91.8 (28.5)	107 (36.1)	104 (32.1)
Median	110	91.1	108	100
(Min, Max)	(55.4, 185)	(31.6, 173)	(29.2, 209)	(29.2, 209)
Brightness Value				
Mean (SD)	7.50 (1.08)	7.21 (0.964)	7.88 (0.968)	7.48 (1.04)
Median	7.70	7.25	7.95	7.60
(Min, Max)	(4.87, 9.16)	(4.98, 9.23)	(5.73, 9.82)	(4.87, 9.82)
Exposure Time				
Mean (SD)	0.00120 (0.00109)	0.00135 (0.00100)	0.000865 (0.000701)	0.00118 (0.000996)
Median	0.000769	0.00105	0.000648	0.000824
(Min, Max)	(0.000279, 0.00546)	(0.000267, 0.00505)	(0.000177, 0.00302)	(0.000177, 0.00546)

Table 3.2: Descriptive statistics of color data and image metadata for anatomic regions and overall. RGB values are calculated by taking the arithmetic means of all 2601 numbers in each color matrix. The higher the RGB value, the stronger the color intensity. The brightness value indicates how bright an image is. The exposure time is the length of time that the digital sensor inside the camera is exposed to light when taking a picture.

			Count of Pictures in Different Regions			
Infant Age (Weeks)	**CBC Hgb Mean (g/dL)**	**CBC Hgb SD (g/dL)**	**Fingernail**	**Palm**	**Toenail**	**All Regions**
0	14.34	3.42	2	2	1	5
1	12.17	2.18	14	12	8	34
2	11.80	1.74	13	8	7	28
3	11.59	1.21	7	6	5	18
4	10.61	1.12	6	11	6	33
5	10.24	1.31	8	7	4	19
6	10.58	1.17	6	7	3	16
7	10.08	0.95	6	5	4	15
8	10.51	1.02	5	9	1	15
9	10.55	1.19	7	2	4	13
10	10.58	1.81	3	2	0	5
11	11.15	1.42	7	3	3	13
12	11.03	1.04	1	3	0	4

SD: standard deviation

Table 3.3: Descriptive statistics of CBC Hgb measurements and number of pictures taken by anatomic regions and in total by infant age in weeks.

	Estimate	Bootstrapped Std. Error	Bootstrapped P-Value
(Intercept)	3.060	4.023	0.444
Fingernail	-	-	-
Palm	-0.646	0.331	0.028
Toenail	0.005	0.380	0.934
R	0.022	0.009	0.020
G	-0.043	0.014	0.002
B	0.021	0.011	0.064
BrightnessValue	0.485	0.404	0.228
ExposureTime	0.390	0.447	0.386
agedays	-0.018	0.007	0.002
gestage	0.161	0.072	0.016

Table 3.4: Linear regression coefficients of the model using the training data from the whole data with anatomic region as a covariate. The training data sample size is 145. Standard errors and p-values are calculated by bootstrapping method for 1000 times. The R squared value of this model is 0.223.

	ModelFingernail	ModelPalm	ModelToenail	Overall
(Intercept)	15.359	9.511	-0.967	3.060
Fingernail	-	-	-	-
Palm	-	-	-	-0.646
Toenail	-	-	-	0.005
R	0.033	0.025	0.011	0.022
G	-0.052	-0.015	-0.016	-0.043
B	0.025	0.001	-0.003	0.021
BrightnessValue	-0.814	0.140	1.022	0.485
ExposureTime	-0.584	0.031	2.122	0.390
agedays	-0.034	-0.013	-0.030	-0.018
gestage	0.041	0.059	0.249	0.161

Table 3.5: Predictive equations of all linear regression models.

	Fingernail Testing Data (n = 25)			Palm Testing Data (n = 23)		
	MSE	MAE	Q2 (Q1, Q3)	MSE	MAE	Q2 (Q1, Q3)
ModelFingernail	3.35	1.48	1.35 (0.39, 2.50)	3.72	1.57	1.36 (0.63, 2.31)
ModelPalm	2.77	1.36	1.15 (0.46, 2.04)	3.10	1.46	1.09 (0.76, 1.86)
ModelToenail	3.89	1.50	1.48 (0.31, 1.92)	6.78	2.18	1.97 (1.25, 2.51)
Overall Model	2.65	1.41	1.24 (0.82, 1.88)	2.58	1.42	1.52 (0.89, 1.87)

	Toenail Testing Data (n = 13)			Whole Testing Data (n = 63)		
	MSE	MAE	Q2 (Q1, Q3)	MSE	MAE	Q2 (Q1, Q3)
ModelFingernail	4.89	1.66	1.18 (0.75, 1.70)	3.39	1.45	1.34 (0.49, 2.14)
ModelPalm	3.48	1.28	0.71 (0.16, 2.53)	3.19	1.33	1.03 (0.50, 1.84)
ModelToenail	5.67	1.99	1.49 (1.01, 2.90)	5.01	1.71	1.36 (0.68, 2.37)
Overall Model	2.55	1.24	0.89 (0.38, 1.66)	2.53	1.26	1.11 (0.55, 1.71)

Table 3.6: Prediction errors of ModelFingernail, ModelPalm, ModelToenail and overall model across all testing data.

Figures

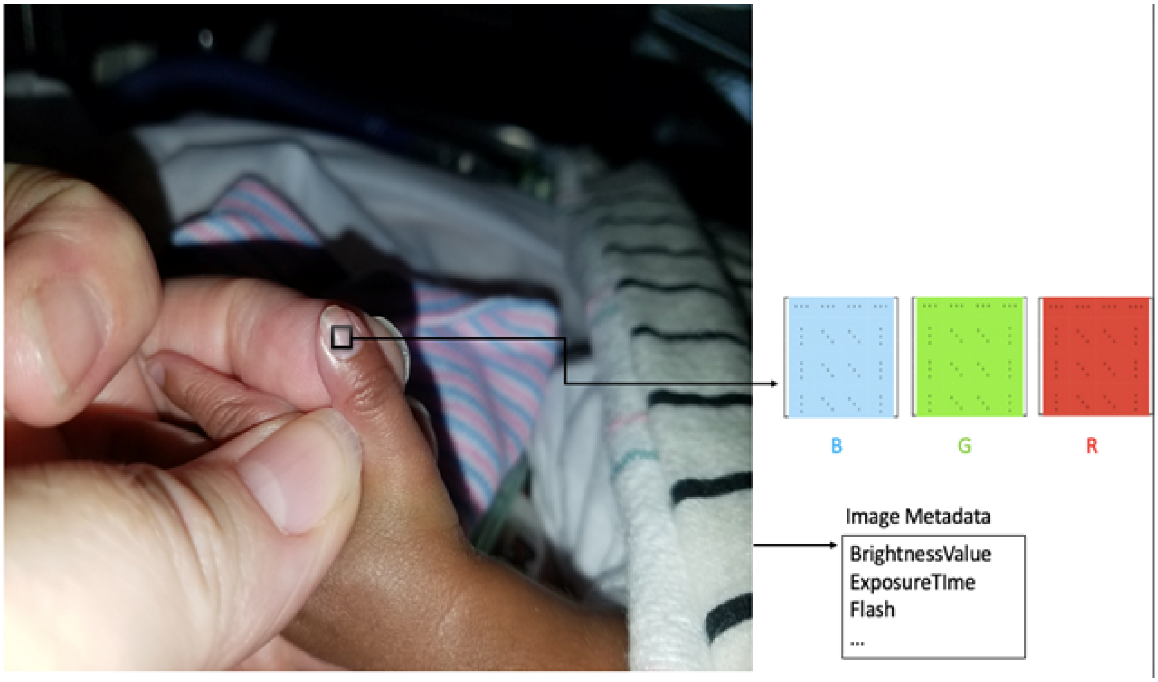

Figure 2.1: Infant 1302471's left fingernail picture taken on October 10th, 2018. Color data were extracted as RGB color data on 51 × 51 pixels.

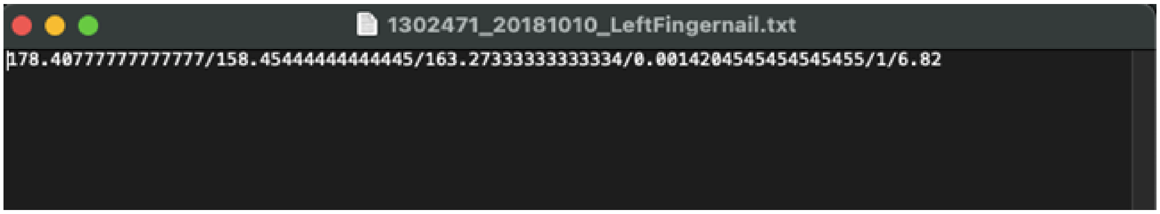

```
178.40777777777777/158.45444444444445/163.27333333333334/0.0014204545454545455/1/6.82
```

Figure 2.2: Infant 1302471's image meta extracted from Dr. Mannino's smartphone app AnemoCheck. Mean RGB of 178.41/158.45/163.27; exposure time of 0.001; flash was used; brightness value 6.82.

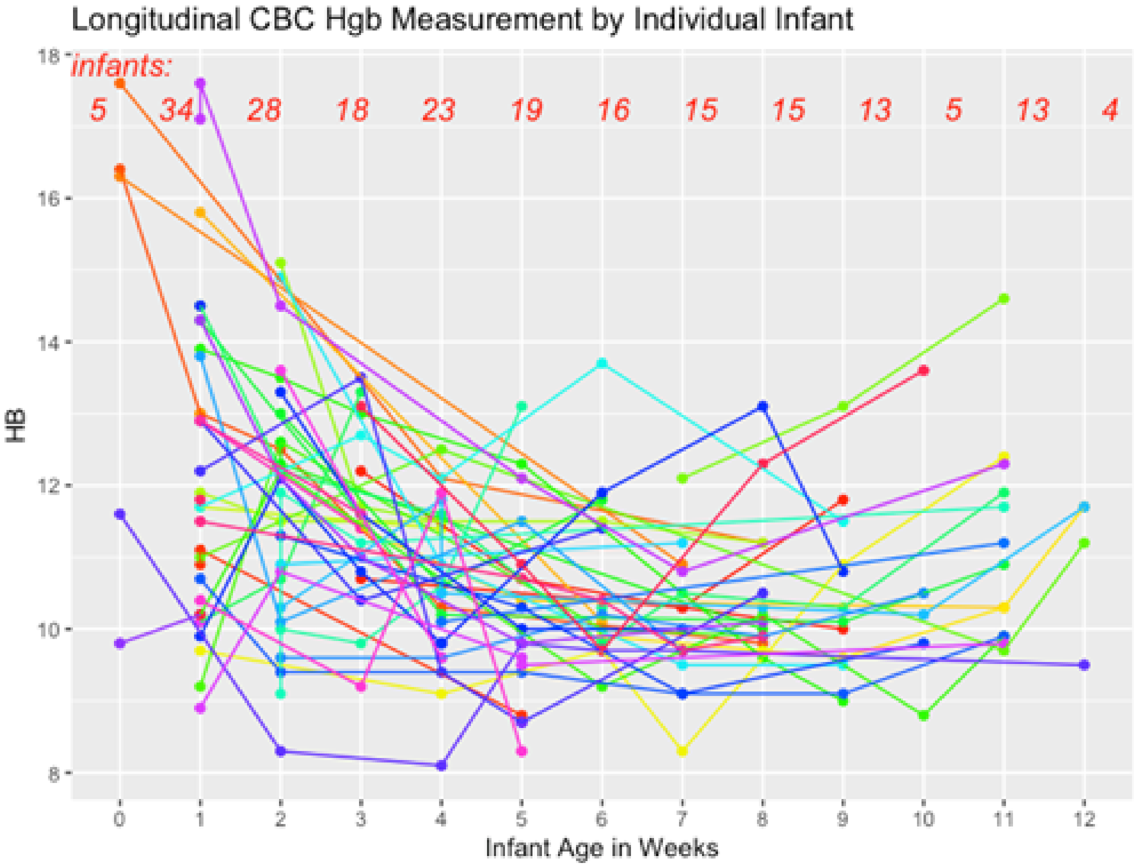

Figure 3.1: Longitudinal CBC Hgb (g/dL) measurements visualization by infant age in weeks in individual level. The number of infants having CBC Hgb levels measured in each week is labeled on the top of the image.

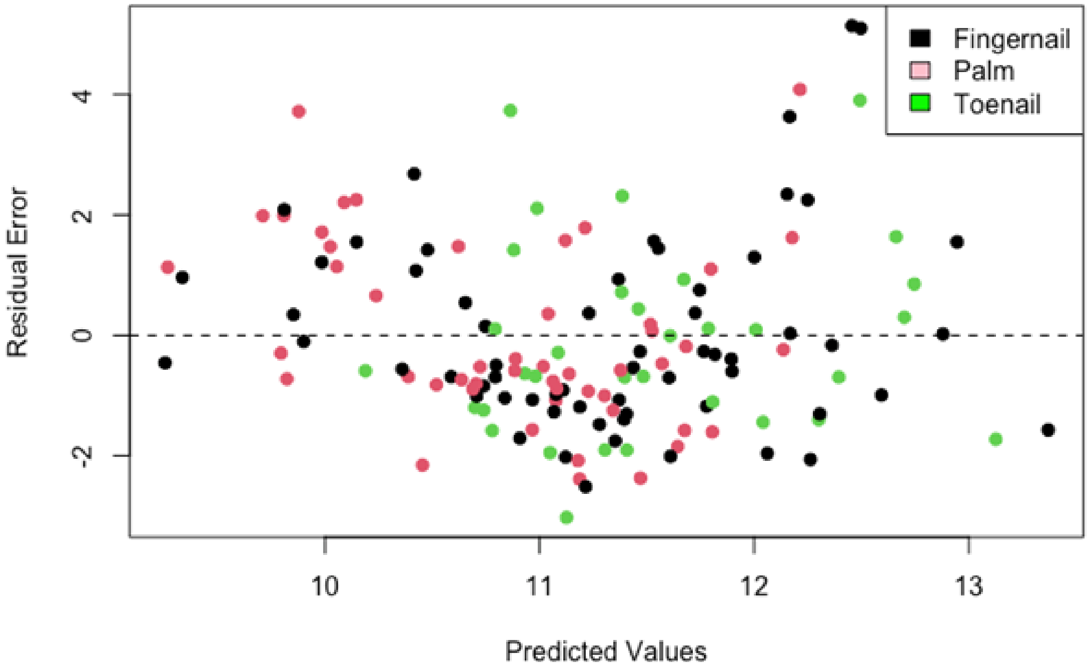

Figure 3.2: Residual error versus predicted values from the model using the training data from the whole dataset for different anatomic regions. Residual errors are calculated by using predicted Hgb levels minus the measured CBC Hgb values.

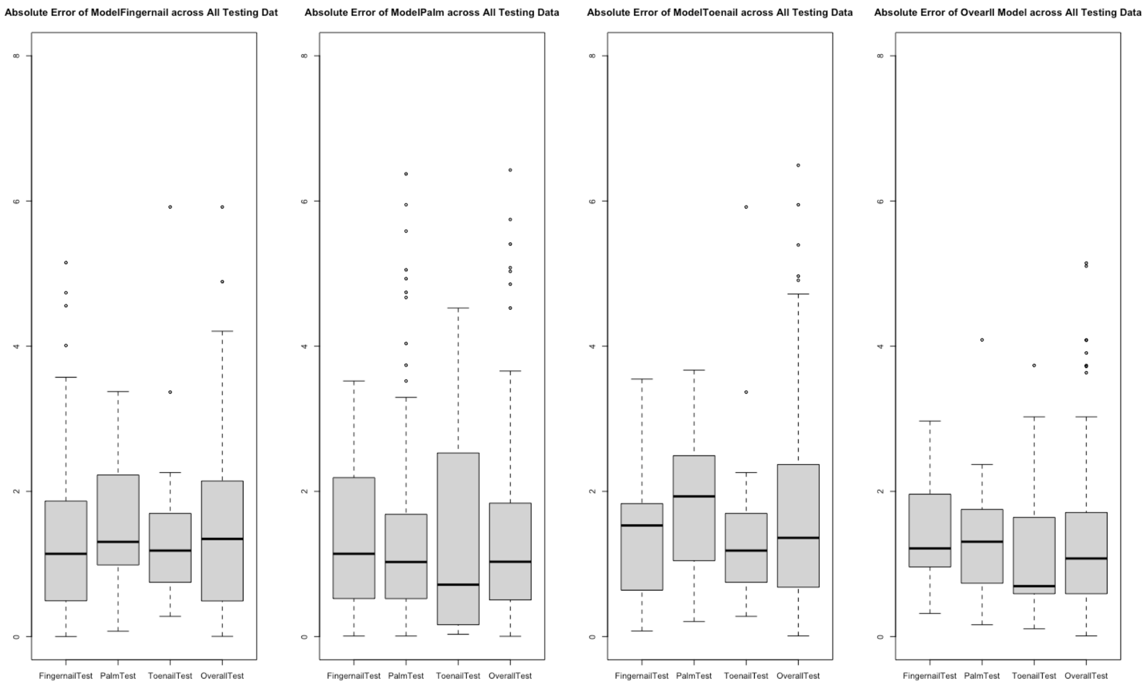

Figure 3.3: Absolute errors for all models (ModelFingernail, ModePalm, ModelToenail and overall model) across all testing data. Absolute errors are displayed in quantiles.

Appendix

	Estimate	Bootstrapped p-values
Intercept	2.557	0.572
Fingernail	-	-
Palm	0.699	0.756
Toenail	4.423	0.086
R	0.028	0.016
G	-0.044	0.002
B	0.025	0.024
BrightnessValue	0.381	0.370
ExposureTime	0.319	0.488
agedays	-0.017	0.004
gestage	0.159	0.030
Palm * R	-0.008	0.552
Toenail * R	-0.026	0.074

Table A0.1: The above regression model adds the two-way interactions between anatomic regions and red color intensity variable for the overall model. The corresponding regression coefficients and bootstrapped p-values are displayed.

	Estimate	Bootstrapped p-values
Intercept	2.916	0.468
Fingernail	-	-
Palm	0.064	0.992
Toenail	2.681	0.080
R	0.022	0.008
G	-0.039	0.002
B	0.026	0.020
BrightnessValue	0.381	0.338
ExposureTime	0.328	0.474
agedays	-0.017	0.004
gestage	0.158	0.030
Palm * G	-0.005	0.658
Toenail * G	-0.022	0.062

Table A0.2: The above regression model adds the two-way interactions between anatomic regions and green color intensity variable for the overall model. The corresponding regression coefficients and bootstrapped p-values are displayed.

	Estimate	Bootstrapped p-values
Intercept	2.688	0.500
Fingernail	-	-
Palm	0.032	0.974
Toenail	1.647	0.210
R	0.022	0.018
G	-0.044	0.002
B	0.029	0.020
BrightnessValue	0.426	0.298
ExposureTime	0.353	0.426
agedays	-0.018	0.012
gestage	0.163	0.018
Palm * B	-0.006	0.676
Toenail * B	-0.015	0.202

Table A0.3: The above regression model adds the two-way interactions between anatomic regions and blue color intensity variable for the overall model. The corresponding regression coefficients and bootstrapped p-values are displayed.

	Estimate	Bootstrapped p-values
Intercept	4.413	0.364
Fingernail	-	-
Palm	-1.968	0.396
Toenail	-2.667	0.354
R	0.022	0.012
G	-0.042	0.008
B	0.021	0.072
BrightnessValue	0.311	0.530
ExposureTime	0.334	0.442
agedays	-0.018	0.008
gestage	0.156	0.026
Palm * BrightnessValue	0.182	0.522
Toenail * BrightnessValue	0.348	0.358

Table A0.4: The above regression model adds the two-way interactions between anatomic regions and brightness variable for the overall model. The corresponding regression coefficients and bootstrapped p-values are displayed.

	Estimate	Bootstrapped p-values
Intercept	3.565	0.382
Fingernail	-	-
Palm	-0.650	0.024
Toenail	-0.055	0.824
R	0.021	0.010
G	-0.041	0.002
B	0.021	0.076
BrightnessValue	0.426	0.278
ExposureTime	0.351	0.316
agedays	-0.018	0.002
gestage	0.160	0.032
Palm * ExposureTime	0.038	0.900
Toenail * ExposureTime	-0.234	0.526

Table A0.5: The above regression model adds the two-way interactions between anatomic regions and exposure time variable for the overall model. The corresponding regression coefficients and bootstrapped p-values are displayed.

	Estimate	Std. Error	t value	Pr(>| t |)	Bootstrapped Std. Error	Bootstrapped P-Value
(Intercept)	15.359	5.356	2.868	0.006	5.308	0.012
R	0.033	0.014	2.277	0.027	0.014	0.018
G	-0.052	0.022	-2.394	0.020	0.020	0.002
B	0.025	0.016	1.557	0.126	0.014	0.034
BrightnessValue	-0.814	0.560	-1.454	0.152	0.548	0.156
ExposureTime	-0.584	0.531	-1.100	0.277	0.554	0.348
agedays	-0.034	0.010	-3.543	0.001	0.010	0.001
gestage	0.041	0.104	0.4397	0.693	0.091	0.640

Table A0.6: Linear regression coefficients and bootstrapping calculated standard errors and p-values of ModelFingernail. The R-squared value for this model is 0.386.

	Estimate	Std. Error	t value	Pr(>| t |)	Bootstrapped Std. Error	Bootstrapped P-Value
(Intercept)	9.511	6.264	1.518	0.136	6.405	0.148
R	0.025	0.017	1.529	0.133	0.016	0.090
G	-0.015	0.022	-0.703	0.495	0.023	0.444
B	-0.001	0.015	-0.046	0.964	0.020	0.958
BrightnessValue	0.140	0.590	0.238	0.813	0.600	0.726
ExposureTime	0.031	0.594	0.052	0.959	0.668	0.908
agedays	-0.013	0.010	-1.308	0.197	0.011	0.148
gestage	0.059	0.116	-0.512	0.611	0.124	0.626

Table A0.7: Linear regression coefficients and bootstrapping calculated standard errors and p-values of ModelPalm. The R-square value of this model is 0.135.

	Estimate	Std. Error	t value	Pr(>| t |)	Bootstrapped Std. Error	Bootstrapped P-Value
(Intercept)	-0.967	9.652	-0.100	0.921	14.78	0.720
R	0.011	0.029	0.383	0.705	0.03	0.614
G	-0.016	0.046	-0.355	0.726	0.05	0.760
B	-0.003	0.036	-0.090	0.930	0.04	0.966
BrightnessValue	1.022	1.052	0.971	0.341	1.76	0.242
ExposureTime	2.122	1.519	1.396	0.175	3.60	0.112
agedays	-0.030	0.017	-1.745	0.094	0.02	0.138
gestage	0.249	0.182	1.369	0.183	0.24	0.220

Table A0.8: Linear regression coefficients and bootstrapping calculated standard errors and p-values of ModelToenail. The R-squared value of this model is 0.387.

References

[1] Claudia Ferri, Renato S. Procianoy, and Rita C. Silveira. Prevalence and risk factors for iron deficiency anemia in very-low-birth-weight preterm infants at 1 year of corrected age. *Journal of Tropical Pediatrics*, 60, February 2014.

[2] John A. Widness. Pathophysiology of anemia during the neonatal period, including anemia of prematurity. *NeoReviews*, 9(11), 2018.

[3] Willemien S. Kalteren, Elise A. Verhagen, Jonathan P. Mintzer, Arend F. Bos, and Elisabeth M. W. Kooi. Anemia and red blood cell transfusions, cerebral oxygenation, brain injury and development, and neurodevelopmental outcome in preterm infants: A systematic review. *Front Pediatr*, 9:644462, 2021.

[4] Andrew M. Freeman, Maitreyee Rai, and Donald W. Morando. *Anemia Screening*. Treasure Island (FL): StatPearls Publishing, 2022.

[5] Mihai Puia-Dumitrescu, David T. Tanaka, Tracy G. Spears, Cecil J. Daniel, Karan R. Kumar, Kamlesh Athavale, Sandra E. Juul, and P. Brian Smith. Patterns of phlebotomy blood loss and transfusions in extremely low birth weight infants. *Journal of perinatology: official journal of the California Perinatal Association*, 39(12):1670–1675, 2019.

[6] Robert G. Mannino, David R. Myers, Erika A. Tyburski, Christina Caruso, Jeanne Boudreaux, Traci Leong, G. D. Clifford, and Wilbur A. Lam. Smartphone app for non-invasive detection of anemia using only patient-sourced photos. *Nat Commun*, 9(4924), 2018.

[7] Juan P Chalco, Luis Huicho, Carlos Alamo, Nilton Y Carreazo, and Carlos A Bada. Accuracy of clinical pallor in the diagnosis of anemia in children: a meta-analysis. *BMC Pediatrics*, 5(46), 2005.

[8] Teresa Oranges, Valentina Dini, and Marco Romanelli. Skin physiology of the neonate and infant: Clinical implications. *Advances in wound care*, 4(10):587–595, 2015.

[9] Starace M., Alessandrini A., and Piraccini B.M. Nail disorders in children. *Skin Appendage Disord*, 4:217–229, 2018.

[10] Ashima Madan, Rahi Kumar, Marian M Adams, William E Benitz, Sharon M Geaghan, and John A Widness. Reduction in red blood cell transfusions using a bedside analyzer in extremely low birth weight infants. *J Perinatol*, 4:21–25, 2005.